DOI: 10.1534/genetics.106.065177

Mutation of a Ubiquitously Expressed Mouse Transmembrane Protein (*Tapt1*) Causes Specific Skeletal Homeotic Transformations

Gareth R. Howell,* Mami Shindo,† Stephen Murray,* Thomas Gridley,* Lawriston A. Wilson* and John C. Schimenti*,[1]

†*Department of Biomedical Sciences, College of Veterinary Medicine, Cornell University, Ithaca, New York 14853 and* **The Jackson Laboratory, Bar Harbor, Maine 04660*

Manuscript received August 22, 2006
Accepted for publication November 21, 2006

ABSTRACT

L5Jcs1 is a perinatal lethal mutation uncovered in a screen for ENU-induced mutations on mouse chromosome 5. *L5Jcs1* homozygotes exhibit posterior-to-anterior transformations of the vertebral column midsection, similar to mice deficient for *Hoxc8* and *Hoxc9*. Positional cloning efforts identified a mutation in a novel, evolutionarily conserved, and ubiquitously expressed gene dubbed *Tapt1* (*Transmembrane anterior posterior transformation 1*). TAPT1 is predicted to contain several transmembrane domains, and part of the gene is orthologous to an unusual alternatively spliced human transcript encoding the cytomegalovirus gH receptor. We speculate that TAPT1 is a downstream effector of HOXC8 that may act by transducing or transmitting extracellular information required for axial skeletal patterning during development.

THE axial skeleton consists of the skull, vertebral column, and thoracic rib cage. The vertebral column contains five types of vertebrae—cervical, thoracic, lumbar, sacral, and caudal—defined by anatomical features and position within the anterior–posterior axis. Variation within the vertebral column plays a significant role in morphological distinctions among species.

In vertebrate embryos, the somites are derived from the paraxial mesoderm and in turn give rise to the sclerotome and the dermomyotome. Chick/quail chimera experiments showed that the sclerotome gives rise to the axial skeleton (Huang *et al.* 2000). Grafting experiments in the chicken demonstrated that posterior portions of the paraxial mesoderm, when transplanted anteriorly, gave rise to posterior structures equivalent to those expected at the original site. Therefore, specification of the vertebral column occurs early in development, prior to the compaction of the paraxial mesoderm into somites (Kieny *et al.* 1972). Key factors known to play a role in this specification are the *Hox* genes. These encode transcription factors that can repress or activate downstream genes. A number of direct targets have been identified, particularly in *Drosophila melanogaster*, but it has been difficult to unequivocally identify mammalian target genes whose expression is directly controlled by Hox genes *in vivo* (Akin and Nazarali 2005; Pearson *et al.* 2005). Chromatin immunoprecipitation and microarray experiments are enabling progress in this area, although potential targets identified require functional validation. Similarly, the mechanisms of Hox gene regulation in mammals are quite complicated, prompting the use of elaborate chromosomal engineering strategies to understand the colinearity of expression within Hox clusters (Tarchini and Duboule 2006). Most of the individual regulators of Hox gene expression remain to be found.

Forward genetic screens are a powerful way to elucidate biological pathways, having the ability to uncover gene–phenotype correlations and developmental hierarchies. Recently, a region-specific ENU mutagenesis screen directed at proximal mouse chromosome 5 yielded 37 embryonic lethal mutations (Wilson *et al.* 2005). Here, we describe the characterization and positional cloning of one of these ENU-induced perinatal lethal mutations (*L5Jcs1*) that causes a homeotic transformation of the axial skeleton similar to that in *Hoxc8* knockout mice (Le Mouellic *et al.* 1992). This novel, ubiquitously expressed gene, which otherwise would not be suspected to yield such a phenotype, uncovers a new aspect of vertebrate axial skeleton patterning.

MATERIALS AND METHODS

Phenotype analysis: The *L5Jcs1* mutation was maintained in *trans* to the Rump white (*Rw*) inversion (for details see Wilson *et al.* 2005). Homozygous embryos or neonates were obtained from intercrossing *Rw/L5Jcs1* mice. Skeletal preparations were based on a published protocol (Kessel and Gruss 1991). Animals were skinned and eviscerated prior to being soaked in 100% ethanol for 4 days. They were then soaked in acetone for 3 days. Animals were rinsed in water and then

[1]*Corresponding author:* Department of Biomedical Sciences, College of Veterinary Medicine, Cornell University, T9014A Vet Research Tower, Ithaca, NY 14853. E-mail: jcs92@cornell.edu

stained (2 vol 0.14% alcian blue (Sigma, St. Louis) in 70% ethanol, 1 vol 0.12% alizarin red (Sigma) in 95% ethanol, 8 vol 100% glacial acetic acid, and 50 vol 70% ethanol) for 10 days. Stain was removed and replaced with 20% glycerol and 1% KOH and incubated at 37° for 16 hr and then at room temperature until the tissue cleared. Preparations were stored in 2:1:1 100% ethanol:glycerol:benzyl alcohol prior to photography.

Mapping *L5Jcs1*: For recombination mapping, *Rw/L5Jcs1* mice were crossed to CAST/Ei, and non-*Rw* F_1 progeny (*L5Jcs1*/CAST) were intercrossed to produce F_2's. These were genotyped with the following polymorphic markers: *D5Mit353*, *D5Mit129*, *D5Mit78*, *D5Mit105*, *D5Mit231*, *D5Mit106*, and *D5Mit107*. The sequences of primer pairs that we developed for mapping deletion breakpoints are as follows: *D5Jcs608*, TAAGTCTGGAGGTGGGGATG and GGCTGTCTTCCTCTC TGTGG; *D5Jcs614*, GCATGAACCTGCACACAGAT and ATGC TGGGAGCAGAACAGTC.

Identification of the *Tapt1* mutation and RT–PCR: RNA was prepared from whole E12.5 embryos using a QIAGEN (Chatsworth, CA) RNeasy kit. Primer pairs used for RT–PCR of the 5′-end of *Tapt1* (*Transmembrane anterior posterior transformation 1*) were Tapt1.1F (CAATGTAGCTTTTAACTCT CACAACA) and Tapt1.1R (TGGCTTCCTTCACGTATTGA). These same primers were used to evaluate tissue-specific expression, using a normalized cDNA panel (BD Biosciences Clontech). Genomic DNA was amplified using the primers Tapt1.G2F (TGACAAAGATGGTATTTCTGTTGC) and Tapt1. G2R (TCAACATTTGCTTATGGTAATGAG) to sequence the mutation.

***In silico* analyses:** Multiple sequence alignments were carried out using ClustalW, and the output was formatted using Multiple Align Show (http://bioinformatics.org/sms/multi_align.html). Programs used to detect potential nuclear localization were PredictNLS (http://cubic.bioc.columbia.edu/predictNLS/) and NucPred (http://www.sbc.su.se/~maccallr/nucpred/). Predicted transmembrane domains were identified by the programs TMPRED (http://www.ch.embnet.org/software/TMPRED_form.html) and TMHMM (http://www.cbs.dtu.dk/services/TMHMM/).

RNA *in situ* hybridization: Embryos were rinsed in 1× phosphate buffered saline (PBS) plus Tween 20 before fixation overnight in 4% paraformaldehyde (PFA). They were then dehydrated by 25, 50, and 75% methanol in PBS before being stored in 100% methanol at −20°. A *Tapt1* riboprobe vector was generated by amplifying a 608-bp RT–PCR product corresponding to nucleotides 1760–2368 of the cDNA, using the following primers that contained SP6 and T7 primer sites, respectively: H3RS7F, GCGATTTAGGTGACACTATAGAATA CTGGATGCTGACACTTGAACA; H3RS7R GCGTAATACG ACTCACTATAGGGAGACCTTTAACTTGGAATAACCAATG. The amplimer was *in vitro* transcribed, incorporating digoxygenin-dUTP.

LacZ staining in *Hoxc8* knockin mice: E12.5 embryos were harvested, rinsed in 1× PBS, and fixed in 4% PFA in PBS at 4° for 5 min. Embryos were stained in X-Gal overnight at 37° and then postfixed in 4% PFA in PBS at 4° overnight. Embryos were placed in 100% glycerol for photography and storage.

RESULTS

The *L5Jcs1* mutation causes homeotic-like transformations of the axial skeleton and perinatal lethality: *L5Jcs1* is one of 37 lethal mutations recovered in a region-specific ENU mutagenesis screen directed at the *Rw* inversion region of proximal mouse chromosome 5 (Wilson *et al.* 2005). The majority of animals homozygous for *L5Jcs1* survived to approximately embryonic day 18.5 (E18.5), but either were born dead or survived until ~1 day postpartum. Newborns or C-section-derived E18.5 homozygous mutants were observed to breath, turn pink, and move actively. Rare homozygotes survived up to several days postpartum, but they were smaller than littermates and never survived to weaning age. The cause of lethality remains unknown (but see DISCUSSION).

As first reported anecdotally (Wilson *et al.* 2005), skeletons from *L5Jcs1/L5Jcs1* mice exhibited certain posterior-to-anterior transformations (Figure 1; Table 1). Specifically, the axial skeleton showed posterior-to-anterior transformations of the thoracic and lumbar vertebrae. Unlike normal mice in which the eighth rib (thoracic segment 8–T8) terminus is free floating, it typically becomes attached to the sixth sternebra in *L5Jcs1* homozygotes. In nearly half the animals, the first lumbar vertebra (L1) showed the development of a 14th pair of ribs. Judging from rib length, it appears that the 9th–13th thoracic vertebrae (T9–13) are transformed into more anterior structures. In addition, the xiphoid process was overgrown and splayed in most mutants (Figure 1, B and C; supplemental Figure 1, B and C, at http://www.genetics.org/supplemental/; Table 1).

Positional cloning of *L5Jcs1*: As previously reported, *L5Jcs1* was never observed to recombine in *trans* to the *Rw* inversion, which spans the ~26- to 74-Mb interval on chromosome 5. The chromosomal deletion $Qdpr^{df3J}$ failed to complement *L5Jcs1* (Wilson *et al.* 2005). Specifically, no *L5Jcs1*/$Qdpr^{df3J}$ weanlings were observed of 23 produced by *Rw/L5Jcs1* × $Qdpr^{df3J}$/+ intercrosses, thus localizing the mutation to this ~15- to 17-Mb interval (Figure 2). To refine the critical region, complementation tests were performed with three other deletions in the *Qdpr* complex: $Qdpr^{df2J}$, $Qdpr^{df6J}$, and $Qdpr^{df11J}$ (Figure 2). None complemented *L5Jcs1*; of the 22, 11, and 31 non-*Rw* progeny, respectively, examined from crosses of each deletion to *L5Jcs1/Rw*, none contained the deletion. This localized the mutation to the 2.5-Mb region between *D5Mit105* and *D5Jcs614*.

To confirm that the failure to obtain *L5Jcs1*/deletion animals was due to noncomplementation rather than to synthetic lethality, timed matings were conducted between $Qdpr^{df2J}$/+ and *Rw/L5Jcs1* mice, and the skeletal phenotypes of three $Qdpr^{df2J}$/*L5Jcs1* E18.5 pups were examined. All three showed the same thoracic rib transformation observed in *L5Jcs1* homozygotes, not only demonstrating that *L5Jcs1* lies within the $Qdpr^{df2J}$ deletion, but also suggesting that it is a null mutation (supplemental Figure 1 at http://www.genetics.org/supplemental/).

To further narrow the interval, recombination mapping was conducted by intercrossing *L5Jcs1*/Cast F_1 heterozygotes and genotyping unaffected F_2 progeny. Regions that were homozygous for the B6 markers could

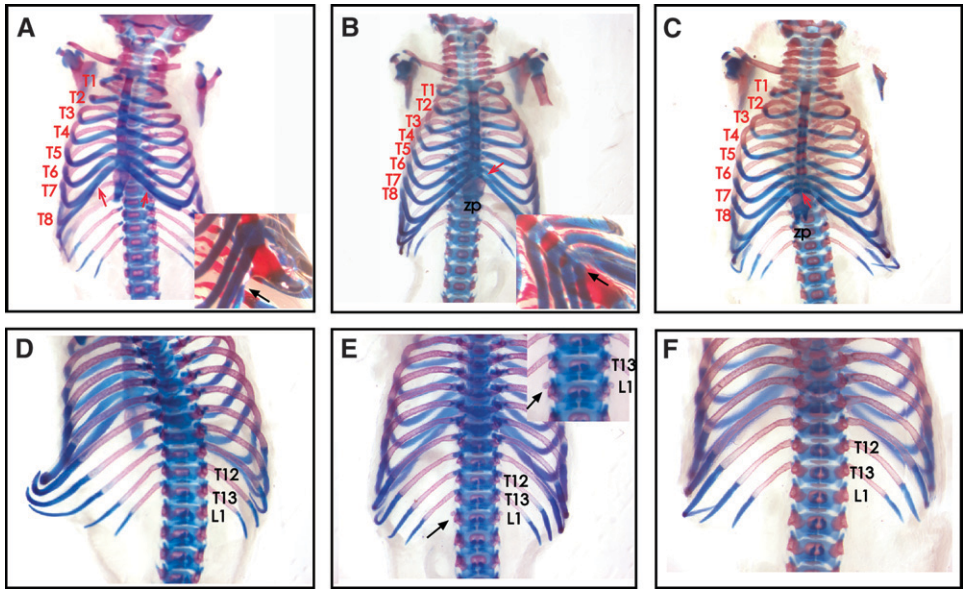

FIGURE 1.—Homeotic-like transformations of *L5Jcs1* skeletons. Shown are E18.5 skeletons stained with alcian blue and alizarin red. The top and bottom rows are ventral and dorsal views, respectively. The lumbar ("L") and thoracic ("T") vertebrae are numbered. (A and D) Wild type. The inset in A is a ventrilateral closeup of T6 and T7 attachment to the sternum; the black arrow points to the terminus of T8, which is unattached to the sternum. (B and E) Homozygous mutant. The inset in B is a ventrilateral closeup of T8 attachment to the sternum (black arrow). The inset in E shows a close-up of the dorsal vertebral column exhibiting partial transformation of L1 into a thoracic-like identity (arrows). (C and F) Homozygous mutant showing the fusion of T8 to the sternum (red arrow in C), but not the L1 partial transformation. Note the splayed xiphoid processes (zp) in B and C.

not contain *L5Jcs1*. These data, combined with data from deletion mapping, localized the mutation to a 1.6-Mb region (between *D5Mit105* and *D5Mit106*) containing 10 Refseq genes (Table 2). Of these, we eliminated several as *L5Jcs1* candidates on the basis of their known mutant phenotypes. Two (*Cd38* and *Ldb2*) have been knocked out in mice, and homozygotes for both are viable. Mutations in *Prom1* cause retinal degeneration in humans, while RNAi inhibition of *Ppih* and 5730509K17Rik in *Caenorhabditis elegans* gives wild-type viable phenotypes.

To identify possible mutations in the remaining six genes, we began generating RT–PCR products from *L5Jcs1/L5Jcs1*, *L5Jcs1/+*, and +/+ E12.5 embryos. No mutations were found in *C1qtnf7*, *Fbxl5*, and *Fgfbp1* (Table 2). In the case of the novel 14-exon mouse gene 4932414K18Rik, a size difference was observed between *L5Jcs1/L5Jcs1* and wild-type-derived products when amplifying between exons 6 and 9. Two bands were observed in heterozygotes (Figure 3A). Sequencing the products revealed that the mutant amplimers lacked exon 7. Analysis of exon 7 and flanking genomic sequence in the mutant revealed a T-to-A transition in the 5′ splice site of intron 7 (3′ of exon 7); this is likely responsible for the skipping of exon 7 during splicing (Figure 3B and Figure 4). This causes an altered reading frame (exon 7 is 70 nucleotides long), resulting in the introduction of 12 anomalous amino acids after N279, followed by a premature termination that probably causes a severe disruption of function. However, the mutant message may also be subject to nonsense-mediated decay; the mutant transcript appears to be present at much lower levels compared to the wild-type transcript in heterozygotes (Figure 3A).

TABLE 1

Penetrance of skeletal abnormalities

Genotype	T8 > T7	L1 > T14	Splayed XP
L1/L1	10/13	6[a]/13	11/13
Rw/+ or L1/+	1/30[b]	1/30[b]	5/30
Fisher's exact test	$P < 0.0001$	$P = 0.00165$	$P < 0.0001$

XP, xiphoid process. L1, *L5Jcs1*. All animals were E18.5–1 day postpartum.

[a] Five of the six had bilateral extra ribs.

[b] The affected animal was exencephalic, and the L1 > T14 transformation was unilateral. This animal also had a splayed XP.

The presence of this mutation in the small, genetically defined mutant interval strongly implicates 4932414K18Rik as *L5Jcs1*. It is unlikely that another locus in the critical region is the causative gene; KEAYS *et al.* (2006) demonstrated that the probability of a cosegregating ENU-induced mutation in a 5-Mb interval (the *Tapt1* interval is only 1.6 Mb) is exceedingly small ($P < 0.002$).

***Tapt1*, the gene mutated in *L5Jcs1*, encodes a highly conserved putative transmembrane protein that overlaps the human cytomegalovirus gH receptor:** 4932414K18Rik encodes a 565-amino-acid protein annotated as LOC231225 in GenBank. Due to the likelihood that mutation of this gene underlies the *L5Jcs1* phenotype, we have renamed it *Tapt1* (*Transmembrane anterior posterior transformation 1*), thus making the allele designation $Tapt1^{L5Jcs1}$.

The predicted TAPT1 protein is evolutionarily conserved. Highly similar orthologs exist from vertebrates to yeast (Figure 4; Figure 5). The overall genomic structure and sequence of *Tapt1* and its vertebrate

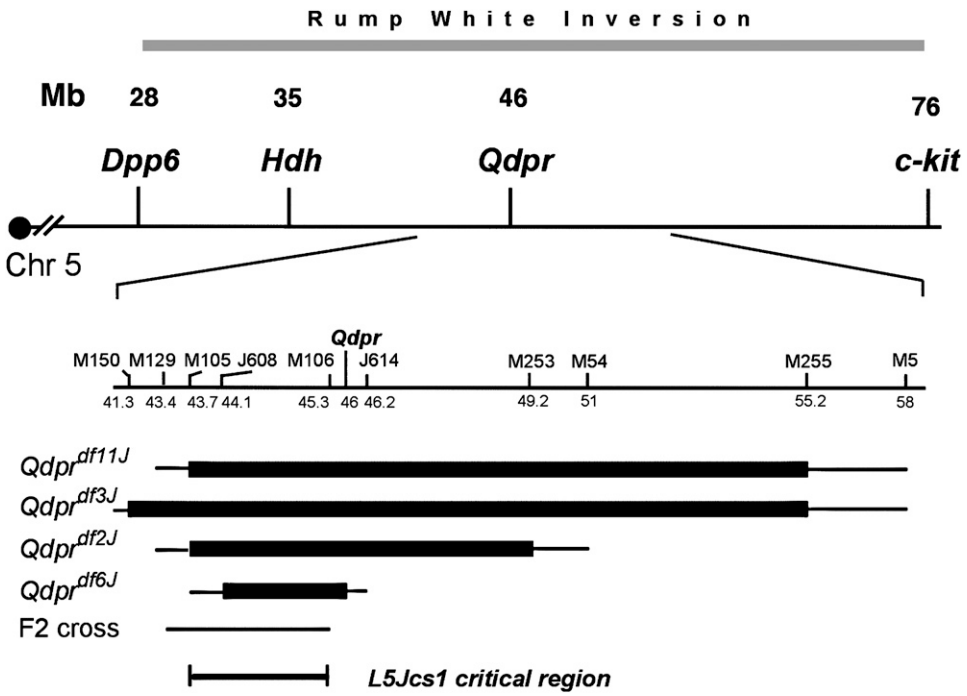

FIGURE 2.—Map of the *L5Jcs1* region. (Top) Map of the *Rw* inversion region of mouse chromosome 5. Some gene loci are indicated. (Bottom) The region surrounding the *Qdpr* deletion complex is expanded. The extents of deletions are indicated as thick horizontal bars. The thinner bars at the ends of the thicker bars indicate the intervals in which the breakpoints lie. The region to which *L5Jcs1* was mapped in the F_2 cross is indicated. Microsatellite loci are abbreviated with the prefix "M" instead of D5Mit. Numbers under these markers are megabase coordinates according to the February 2006 mouse genome assembly Build 36. The *L5Jcs1* critical region is indicated.

orthologs are conserved (Figure 4). A variety of ESTs led to the derivation of a consensus RefSeq structure for mouse *Tapt1*, with the exception of one alternatively spliced 66-bp exon that is present in some ESTs and that corresponds to conserved vertebrate sequences in homology plots (Figure 4).

The intron/exon structure of the human ortholog aligns well with mouse, with the exception of AF189251, a cDNA corresponding to exon 1, part of exon 4, and a portion of intron 4, in which it terminates. This cDNA was reported to encode the human cytomegalovirus (HCMV) gH receptor (BALDWIN *et al.* 2000). A BLAST search of the mouse TAPT1 amino acid sequence against human proteins revealed a high similarity to that part of the AF189251 protein encoded by exons 1 and 4. However, our analysis with the now-available human genome sequence shows that much of the predicted AF189251 protein corresponds to that encoded by the intron 4 sequence. Interestingly, this intron-4-encoded amino acid sequence includes the receptor for the HCMV gH glycoprotein ligand and is essential for virus infectivity (BALDWIN *et al.* 2000). The ability of anti-AF189251 monoclonal antibodies to block viral infection provides experimental support for the prediction that the intron-4-encoded epitopes of the protein are present at the cell surface (BALDWIN *et al.* 2000), but it is not clear which amino acids are responsible for placing the protein at the cell surface. Interestingly, the AF189251 cDNA is unique; no mouse or human ESTs exhibit a similarly spliced form. Furthermore, VISTA analysis (MAYOR *et al.* 2000) indicates that the intron-4-coding region is not evolutionarily conserved (not shown).

Other than this unusual AF189251 transcript, no other information on the cellular function of mammalian TAPT1 exists. Analysis with the TMPRED and TMHMM protein analysis algorithms indicates that TAPT1 contains as many as six transmembrane domains (supplemental Figure 2 at http://www.genetics.org/supplemental/). Alignment of the predicted amino acid sequence reveals high levels of conservation from mammals to yeast, especially near its central region

TABLE 2

Genes in the *L5Jcs1* critical region

Gene	Exons	KO	Sequenced
C1qtnf7 (C1q and TNF-related protein 7)	6		Yes
5730509K17Rik	40		
Fbxl5 (F-box and leucine-rich-repeat protein 5)	9		Yes
Bst1 (bone marrow stromal antigen 1)	9		Yes[c]
Cd38	8	Yes[a]	
Ppih (peptidyl prolyl isomerase H)	1		
Fgfbp1 (fibroblast growth factor binding protein 1)	2		Yes
Prom1 (prominin 1)	27		
4932414K18Rik (*Tapt1*)	14		Yes
Ldb2 (LIM homeodomain binding 2)	9	Yes[b]	

C1qtnf7 is subject to alternative splicing; all isoforms were sequenced. Primers used for sequencing are in supplemental Table 1 at http://www.genetics.org/supplemental/. KO, knockout allele available.

[a] Mutants are viable.

[b] A Lexicon viable mutant.

[c] All coding regions but exon 5 were sequenced.

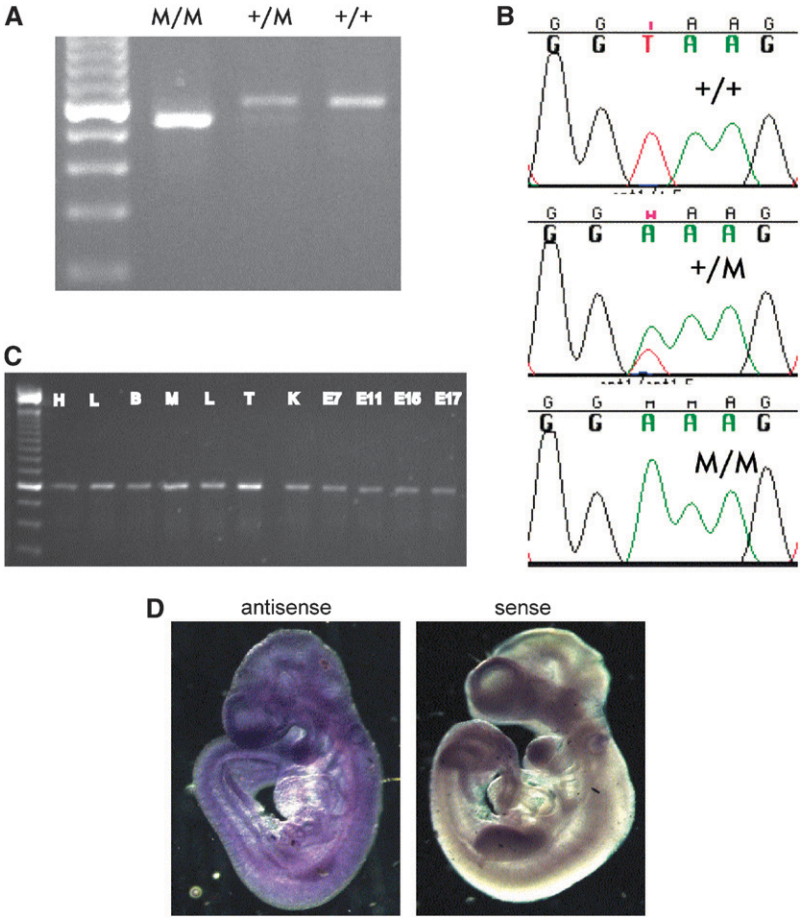

FIGURE 3.—Identification of mutation in *Tapt1* and RT–PCR analysis. (A) RT–PCR analysis of the *Tapt1* gene using primers flanking exon 7. M, mutant (*L5Jcs1* allele). Note the fainter mutant (lower) band in the heterozygote. The leftmost lane is a 100-bp ladder. (B) DNA sequence traces of indicated genotypes of the distal exon 7 splice junction. (C) PCR analysis of cDNAs from various tissues. (D) *In situ* hubridization of antisense or sense (control) RNAs to E9.5 wild-type embyros. H, heart; L, lung; B, brain; M, skeletal muscle; L, liver; T, testis; K, kidney; E, embryonic day.

(Figure 5). The *L5Jcs1* mutation lies within this highly conserved region, near the end of a 133-amino-acid stretch that (with one residue exception) is perfectly identical among humans, mice, chickens, and zebrafish.

Yeast deleted for their *Tapt1* ortholog (an uncharacterized ORF called YER140W) are viable, although *C. elegans* RNA interference (RNAi) screens (summarized in WormBase) report that one of five RNAi molecules directed against the worm ortholog cause 24–100% embryonic lethality. The YER140W gene product was found to interact, in two-hybrid screens, with Mch1p, Dhh1p, and Tma19p (ITO *et al.* 2001). Mch1p has similarity to mammalian monocarboxylate permeases, which are involved in transport of monocarboxylic acids across plasma membranes. However, *mch1* mutants are not deficient in monocarboxylic acid transport (MAKUC *et al.* 2001). Dhh1p is a putative DexD/H-box helicase, involved in mRNA export and translation. *TMA19* is a nonessential gene encoding a putative ribosomal protein (according to the Saccharomyces Genome Database). In sum, while there have been no directed studies of *Tapt1* or its homologs in experimental organisms, evidence suggests that it is a transmembrane protein involved in transporting molecules across membranes and may be required for normal embryonic development in both worms and mice.

***Tapt1* expression:** Despite the specific skeletal defect exhibited by mutant embryos, *Tapt1* is widely expressed. Public databases contain 223 *Tapt1* ESTs stemming from 30 different cDNA libraries, according to Unigene and the Stanford S.O.U.R.C.E. (DIEHN *et al.* 2003). We conducted RT–PCR analysis to confirm the apparently ubiquitous pattern of *Tapt1* expression in both adult tissues and whole E7–E17 embryos (Figure 3C). All samples yielded similar amounts of *Tapt1* product from normalized cDNA sources (see MATERIALS AND METHODS). To determine if *Tapt1* is expressed in distinct embryonic structures that might correspond to the observed skeletal defects, whole-mount RNA *in situ* hybridization was performed on E9.5 embryos. *Tapt1* message, as detected by two nonoverlapping probes (Figure 3D; data not shown), was present throughout the embryo.

Hox gene expression in *L5Jcs1* mutants: This skeletal phenotype is remarkably similar to mice with a knockout of *Hoxc8*, and to a somewhat lesser degree, *Hoxc9* (LE MOUELLIC *et al.* 1992; SUEMORI *et al.* 1995). Mutations in genes that cause axial skeletal patterning defects typically disrupt the expression pattern of a Hox gene(s) that, when mutated, causes a similar phenotype (see DISCUSSION). We therefore explored whether mutation of *Tapt1* disrupts *Hoxc8* expression, exploiting an allele of *Hoxc8* containing a knocked-in LacZ reporter

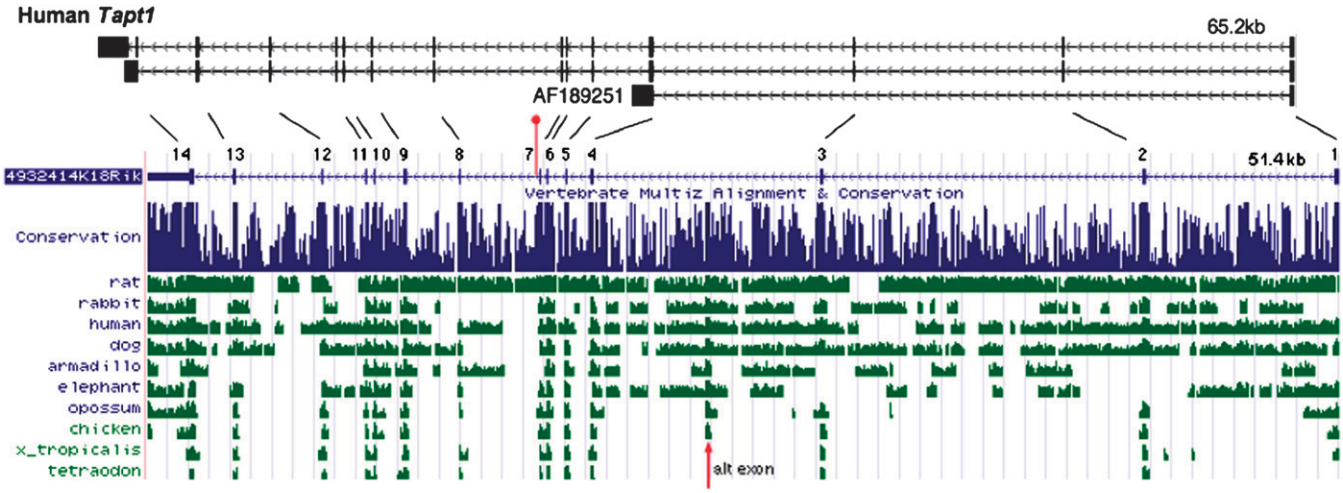

FIGURE 4.—Structure of the mouse and human Tapt1 genes. The genomic structures of mouse *Tapt1* (4932414K18Rik) and human *Tapt1* (FLJ90013), as represented in the University of California at Santa Cruz (UCSC) Genome Browser as of April 2006 are shown, as are three human mRNAs from GenBank. The AF189251 mRNA was reported to encode the HCMV gH receptor (BALDWIN *et al.* 2000). Exons are represented by vertical bars along the horizontal lines and are numbered. Transcription is to the left, toward the centromere in both species. The location of the *L5Jcs1* mutation, distal to exon 7, is indicated by a vertical red bar/ball. The lines drawn between the human and mouse genes connect orthologous exons. (Bottom) A depiction of conservation between the mouse sequence and other vertebrates, as displayed by the indicated UCSC browser track. The red arrow indicates the location of a highly conserved region that corresponds to an alternative exon included in some ESTs (not shown).

that is expressed in a pattern that reflects endogenous *Hoxc8* transcription (LE MOUELLIC *et al.* 1992). Double heterozygotes (*L5Jcs1*/+; *Hoxc8*−/+) were crossed to *L5Jcs1* heterozygotes, and the embryos were stained for LacZ and genotyped. There was no alteration in LacZ expression in embryos homozygous for the *L5Jcs1* mutation and that contained the *Hoxc8* allele (Figure 6).

DISCUSSION

Function of TAPT1 in development: All or most known mouse mutations that cause homeotic skeletal transformations either are in the Hox genes themselves or affect Hox gene expression. The latter include polycomb and trithorax genes (HANSON *et al.* 1999), the *E2f6* transcription factor (STORRE *et al.* 2002), the homeobox gene *Cdx1* (SUBRAMANIAN *et al.* 1995), the TGF-β family member *Bmp11* (MCPHERRON *et al.* 1999), *Plzf* (BARNA *et al.* 2000), and others (VAN DER LUGT *et al.* 1996; OH and LI 1997; COLLINS *et al.* 2002). The TAPT1 protein sequence itself does not contain any apparent nuclear localization signals or DNA-binding motifs, suggesting that it does not directly modulate gene expression. Indeed, we found that *Hoxc8* expression appeared unaffected in *L5Jcs1* mutants, although it remains possible that TAPT1 affects the expression of other Hox genes. Thus, it appears that TAPT1 functions at a unique level in the regulatory hierarchy of axial skeletal patterning among molecules known to be involved in the process.

The most enigmatic aspect of *Tapt1* is that its mutation causes a specific developmental defect yet its expression is widespread. There are at least two models that we can envision to reconcile this paradox. One is that TAPT1 is a ubiquitously expressed receptor that enables developmentally specific functions by transducing extracellular signals that are acted upon by effectors downstream of Hox genes. Specificity of action at particular times and places during development would be conferred by the ligands. The idea that TAPT1 is a cell surface receptor is consistent with the presence of several transmembrane domains and with the fact that an alternatively spliced human ortholog encodes the HCMV gH cell surface receptor (with many caveats related to the "normal" TAPT1 as discussed below).

The second model is that *Tapt1* is not truly ubiquitously expressed during development, but rather its expression is modulated in certain cell types at particular times that are important in patterning the skeleton. The Hox family of transcription factors is the most well-studied group of genes affecting segmental identity of the axial skeleton (reviewed by FAVIER and DOLLE 1997). In mouse, the Hox genes are expressed in partially overlapping regions including mesoderm, neuroectoderm, and endoderm from the base of the head to the tail. As indicated earlier, disruption of both *Hoxc8* and *Hoxc9*leads to posterior-to-anterior transformations of the thoracic and lumbar vertebrae similarly to *L5Jcs1*, that is, attachment of T8 to the sternum, formation of a partial 14th pair of ribs on the first lumbar segment, and a malformed xiphoid process (LE MOUELLIC *et al.* 1992; SUEMORI *et al.* 1995). In addition to other axial skeleton abnormalities, *Hoxc4* mutant mice often display the T8 sternum attachment and xiphoid process malformations similarly to *L5Jcs1* homozygotes (SAEGUSA *et al.*

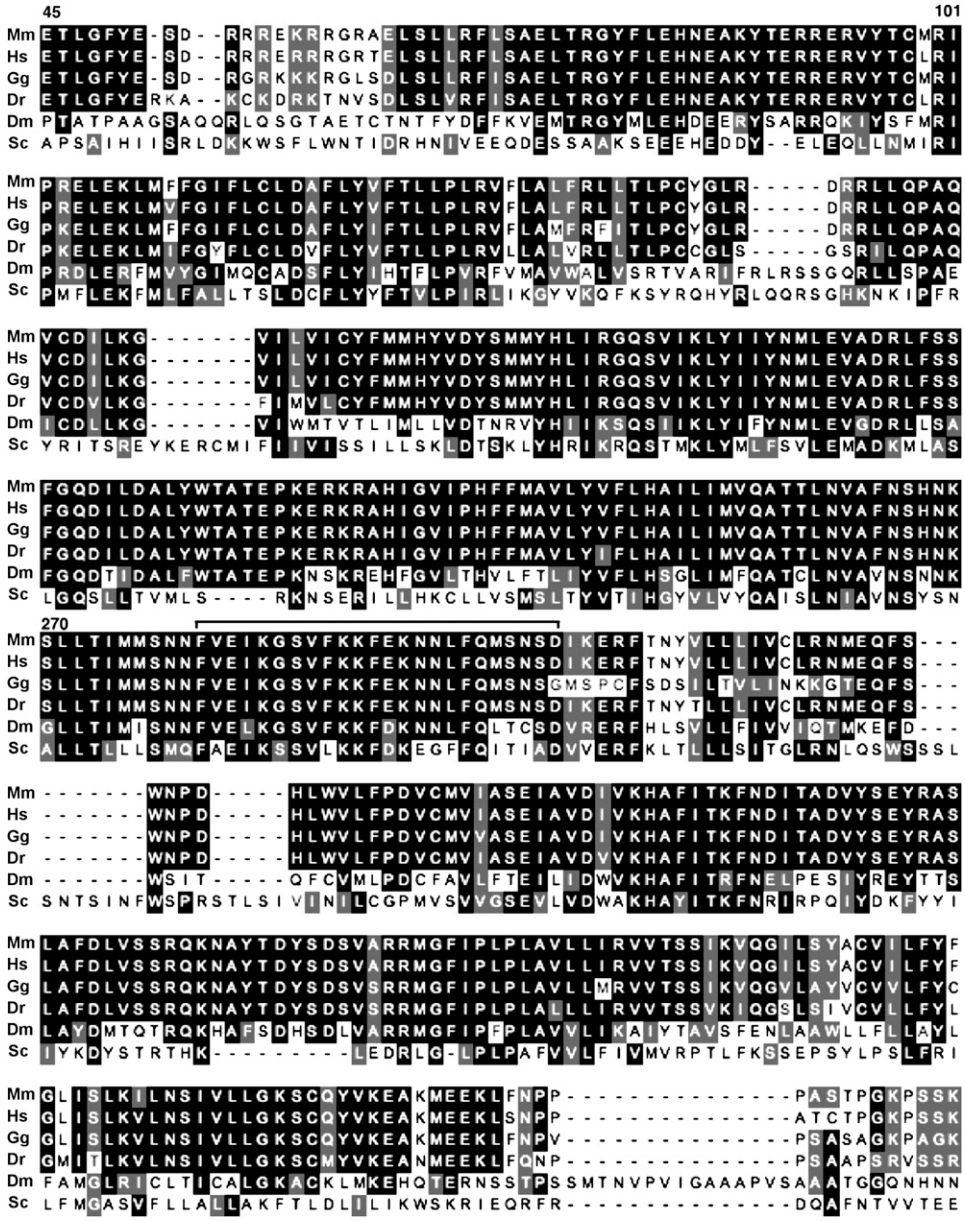

FIGURE 5.—Alignment of TAPT1 orthologs. Identical amino acids are on a black background only in those cases where four or more residues have identity or similarity. Similar residues are shaded. The amino and carboxy terminal ends of the proteins, where homology decays markedly, are not aligned here. Some landmark amino acid positions in mice are indicated. Dashes are introduced to maximize alignment by the ClustalW algorithm. A bracket above the sequence corresponds to those amino acids encoded by mouse exon 7, which is skipped in the *L5Jcs1* allele. Mm, mouse; Hs, human; Gg, chicken; Dr, zebrafish; Dm, *D. melanogaster*; Sc, *Saccharomyces cerevisiae*.

1996). The *L5Jcs1* phenocopy raises the possibility that one or more Hox genes regulate the pattern of *Tapt1* in development and that *Tapt1*, possibly acting at the cell surface, affects specification of developing axial skeletal components.

Progress in identifying downstream targets of HOX proteins in mice has been limited. Notably, LEI *et al.* (2005) identified potential targets of *Hoxc8* regulation by overexpressing *Hoxc8* in mouse embryonic fibroblasts and then performing microarray analysis. They identified 34 genes that were up-or downregulated, but none were *Tapt1*.

Other roles in homeostasis and development: A major unanswered question about the biological role(s) of *Tapt1* concerns the cause of lethality. It is unlikely to be due to the skeletal defects *per se*, since mice with similar transformations (such as *Hoxc8*$^{-/-}$) can be viable and fertile. Because the gene is expressed ubiquitously, defects in other tissues are probably responsible. In an attempt to gain insight into the cause of death, we completely sectioned the head and thoracic region of a single mutant sickly animal that survived 3 days postpartum. Abnormalities noted were an infarction in brain, nasal congestion, pneumonia, and a potential swelling of heart vessels that might underlie the other phenotypes. Additional work will reveal if these defects are direct manifestations of the *L5Jcs1* mutation.

On the role of *TAPT1* as a HCMV receptor: A very interesting finding is that an unusual isoform of the human *TAPT1* gene encodes the HCMV gH receptor. The identity of this receptor was uncovered by screening of cDNA expression libraries with monoclonal antibodies against the gH receptor (BALDWIN *et al.* 1996, 2000). The DNA sequences of these clones were

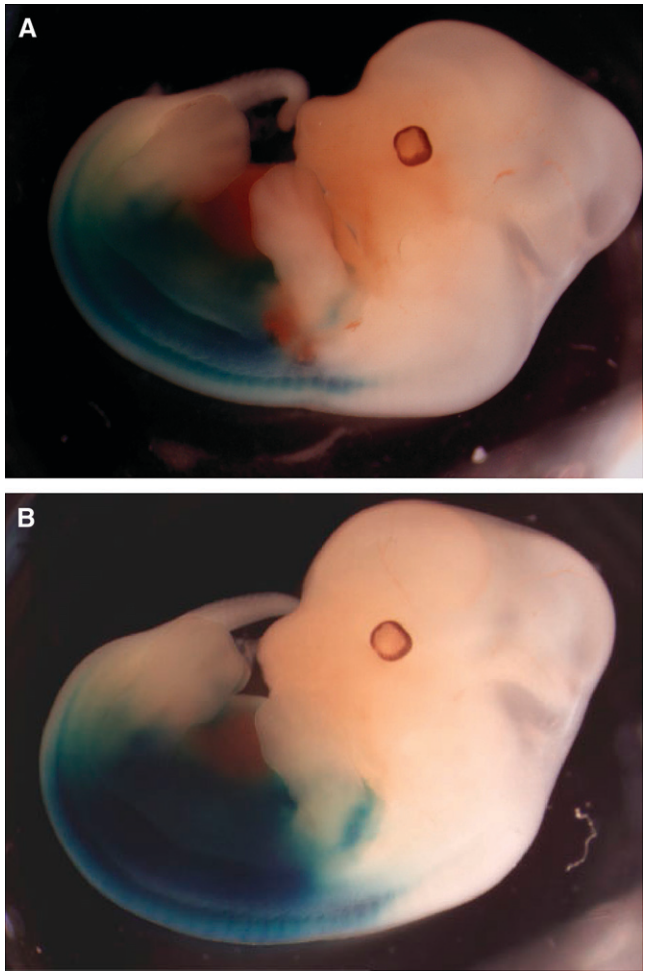

FIGURE 6.—*Hoxc8* expression in *L5Jcs1* mutant and control embryos. Shown are whole-mount E12.5 embryos stained for LacZ activity. The LacZ gene is under the control of the *Hoxc8* promoter. (A) *L5Jcs1*/+; *Hoxc8*$^{+/-}$. (B) *L5Jcs1*/*L5Jcs1*; *Hoxc8*$^{+/-}$.

determined before the human genome sequence and EST collections were available. As we describe in the RESULTS, the clones identified by BALDWIN and colleagues represent an alternatively spliced form of TAPT1 that is not found in any EST sequenced to date. Given that only three clones containing this gH receptor isoform were identified from two human embryonic lung cell cDNA libraries, it is likely that this is an extremely rare isoform and/or is restricted to a small number of tissues.

Our observation that much of the HCMV coding region lies in what is an intron with respect to the "normal" transcription unit, and that this region is apparently not conserved, raises interesting questions about the mechanisms by which receptors for pathogens can arise. One possibility is that this alternative coding region predated the mammalian radiation, serving some function that became important exclusively for humans, only to be exploited by CMV after the divergence of species. Alternatively, it may have arisen in the primate lineage and fortuitously (for CMV) encoded a protein variant (essential or not) that CMV exploited.

During the course of scrutinizing the amino acid sequence of TAPT1 for similarity to known conserved motifs using Pfam, we noted that unfortunately this database lists the central half of the sequence as being a member of the "DUF747, eukaryotic membrane protein (cytomegalovirus gH-receptor) family." However, most of this DUF747 region consists of amino acids that are not encoded by the gH receptor cDNA isoform, but rather correspond to the highly conserved region of mouse TAPT1 stretching from residues 148 to 459. This annotation is therefore potentially very misleading to those studying any of the TAPT1 orthologs. There are no apparent paralogs in the mouse genome.

The authors thank Tim O'Brien for experimental advice and Rod Bronson for evaluation of pathology. This work was funded by grant HD35984 to J.C.S. from the National Institute of Child Health and Human Development.

LITERATURE CITED

AKIN, Z. N., and A. J. NAZARALI, 2005 Hox genes and their candidate downstream targets in the developing central nervous system. Cell. Mol. Neurobiol. **25:** 697–741.

BALDWIN, B., M. KLEINBERG and S. KEAY, 1996 Molecular cloning and expression of receptor peptides that block human cytomegalovirus/cell fusion. Biochem. Biophys. Res. Commun. **219:** 668–673.

BALDWIN, B., C. ZHANG and S. KEAY, 2000 Cloning and epitope mapping of a functional partial fusion receptor for human cytomegalovirus gH. J. Gen. Virol. **81:** 27–35.

BARNA, M., N. HAWE, L. NISWANDER and P. P. PANDOLFI, 2000 Plzf regulates limb and axial skeletal patterning. Nat. Genet. **25:** 166–172.

COLLINS, E. C., A. APPERT, L. ARIZA-MCNAUGHTON, R. PANNELL, Y. YAMADA *et al.*, 2002 Mouse Af9 is a controller of embryo patterning, like Mll, whose human homologue fuses with Af9 after chromosomal translocation in leukemia. Mol. Cell. Biol. **22:** 7313–7324.

DIEHN, M., G. SHERLOCK, G. BINKLEY, H. JIN, J. C. MATESE *et al.*, 2003 SOURCE: a unified genomic resource of functional annotations, ontologies, and gene expression data. Nucleic Acids Res. **31:** 219–223.

FAVIER, B., and P. DOLLE, 1997 Developmental functions of mammalian Hox genes. Mol. Hum. Reprod. **3:** 115–131.

HANSON, R. D., J. L. HESS, B. D. YU, P. ERNST, M. VAN LOHUIZEN *et al.*, 1999 Mammalian Trithorax and polycomb-group homologues are antagonistic regulators of homeotic development. Proc. Natl. Acad. Sci. USA **96:** 14372–14377.

HUANG, R., Q. ZHI, C. SCHMIDT, J. WILTING, B. BRAND-SABERI *et al.*, 2000 Sclerotomal origin of the ribs. Development **127:** 527–532.

ITO, T., T. CHIBA, R. OZAWA, M. YOSHIDA, M. HATTORI *et al.*, 2001 A comprehensive two-hybrid analysis to explore the yeast protein interactome. Proc. Natl. Acad. Sci. USA **98:** 4569–4574.

KEAYS, D. A., T. G. CLARK and J. FLINT, 2006 Estimating the number of coding mutations in genotypic- and phenotypic-driven N-ethyl-N-nitrosourea (ENU) screens. Mamm. Genome **17:** 230–238.

KESSEL, M., and P. GRUSS, 1991 Homeotic transformations of murine vertebrae and concomitant alteration of Hox codes induced by retinoic acid. Cell **67:** 89–104.

KIENY, M., A. MAUGER and P. SENGEL, 1972 Early regionalization of somitic mesoderm as studied by the development of axial skeleton of the chick embryo. Dev. Biol. **28:** 142–161.

LEI, H., H. WANG, A. H. JUAN and F. H. RUDDLE, 2005 The identification of Hoxc8 target genes. Proc. Natl. Acad. Sci. USA **102:** 2420–2424.

Le Mouellic, H., Y. Lallemand and P. Brulet, 1992 Homeosis in the mouse induced by a null mutation in the Hox-3.1 gene. Cell **69:** 251–264.

Makuc, J., S. Paiva, M. Schauen, R. Kramer, B. Andre *et al.*, 2001 The putative monocarboxylate permeases of the yeast Saccharomyces cerevisiae do not transport monocarboxylic acids across the plasma membrane. Yeast **18:** 1131–1143.

Mayor, C., M. Brudno, J. R. Schwartz, A. Poliakov, E. M. Rubin *et al.*, 2000 VISTA: visualizing global DNA sequence alignments of arbitrary length. Bioinformatics **16:** 1046–1047.

McPherron, A. C., A. M. Lawler and S. J. Lee, 1999 Regulation of anterior/posterior patterning of the axial skeleton by growth/differentiation factor 11. Nat. Genet. **22:** 260–264.

Oh, S. P., and E. Li, 1997 The signaling pathway mediated by the type IIB activin receptor controls axial patterning and lateral asymmetry in the mouse. Genes Dev. **11:** 1812–1826.

Pearson, J. C., D. Lemons and W. McGinnis, 2005 Modulating Hox gene functions during animal body patterning. Nat. Rev. Genet. **6:** 893–904.

Saegusa, H., N. Takahashi, S. Noguchi and H. Suemori, 1996 Targeted disruption in the mouse Hoxc-4 locus results in axial skeleton homeosis and malformation of the xiphoid process. Dev. Biol. **174:** 55–64.

Storre, J., H. P. Elsasser, M. Fuchs, D. Ullmann, D. M. Livingston *et al.*, 2002 Homeotic transformations of the axial skeleton that accompany a targeted deletion of E2f6. EMBO Rep. **3:** 695–700.

Subramanian, V., B. I. Meyer and P. Gruss, 1995 Disruption of the murine homeobox gene Cdx1 affects axial skeletal identities by altering the mesodermal expression domains of Hox genes. Cell **83:** 641–653.

Suemori, H., N. Takahashi and S. Noguchi, 1995 Hoxc-9 mutant mice show anterior transformation of the vertebrae and malformation of the sternum and ribs. Mech. Dev. **51:** 265–273.

Tarchini, B., and D. Duboule, 2006 Control of Hoxd genes' collinearity during early limb development. Dev. Cell **10:** 93–103.

van der Lugt, N. M., M. Alkema, A. Berns and J. Deschamps, 1996 The Polycomb-group homolog Bmi-1 is a regulator of murine Hox gene expression. Mech. Dev. **58:** 153–164.

Wilson, L., Y.-H. Ching, M. Farias, S. A. Hartford, G. Howell *et al.*, 2005 Random mutagenesis of proximal mouse chromosome 5 uncovers predominantly embryonic lethal mutations. Genome Res. **15:** 1095–1105.

Communicating editor: K. V. Anderson